Supplementary information 1 for ”Vibrational Contribution to the Sub-Terahertz Dielectric Response of Kinesin and Its Hydration Shell”

Saurabh K. Pandey[1] **and Michal Cifra**[1,*]

[1]Institute of Photonics and Electronics of the Czech Academy of Sciences, Prague, Czechia
[*]cifra@ufe.cz

ABSTRACT

-

S1-1 Dipole Variation and Absorption Behavior of Kinesin and Tubulin under Hydration and Damping Effects

Figures S1-1–S1-3 summarize the variation of mode-resolved dipole moments and the corresponding absorption characteristics for kinesin and tubulin systems under different hydration and damping conditions. Figure S1-1 compares the first ten vibrational modes of kinesin in the dry (0 Å) and hydrated (3 Å) states, showing that hydration slightly reduces the average dipole strength while preserving the overall frequency distribution. Each colored dot represents a single mode from one of the 92 molecular models, whereas the larger outlined circles denote the mean dipole values across all models for a given mode. Extending the analysis to the first thousand modes, Figure S1-2 displays the dipole variation for kinesin and tubulin systems with a 3 Å hydration shell. The scatter plots reveal a broad spread of dipole magnitudes with frequency, while the overlaid mode-count curves indicate that tubulin exhibits a higher density of modes in the sub-terahertz region compared with kinesin. This suggests that tubulin possesses a richer distribution of low-frequency collective motions contributing to its dielectric response. Finally, Figure S1-3 presents the computed absorption spectra of hydrated kinesin and tubulin for different damping factors ($\gamma = 10$–$10{,}000$ GHz). The spectra exhibit a monotonic increase in absorption with both frequency and damping. Tubulin consistently shows higher absorption coefficients than kinesin, reflecting its larger dipole variability and greater mode density. Together, these results demonstrate how hydration and molecular damping jointly modulate the protein-level dielectric and absorptive behavior across the gigahertz-to-terahertz frequency range.

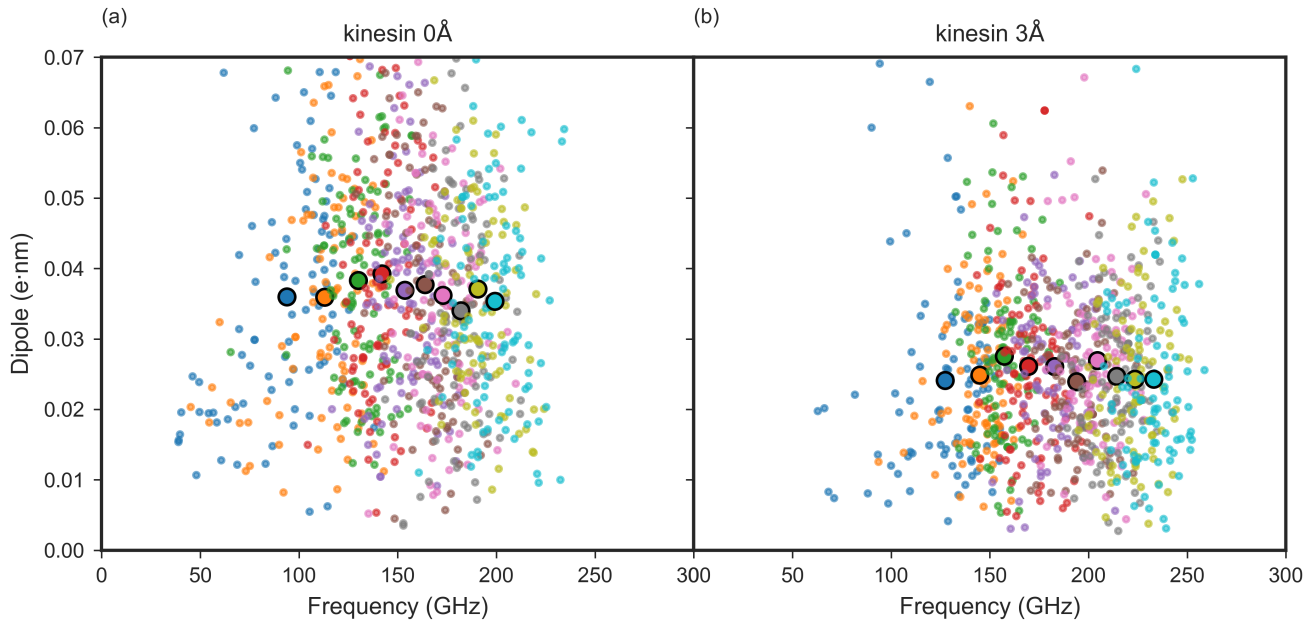

Figure S1-1. Comparison of variation of dipole of kinesin 0 Å and kinesin 3 Å system, showing ρ over frequency for first ten modes. Each small dot represents the dipole moment and frequency of a given mode from one of the 92 models, while the larger outlined circles indicate the average values over all models for each mode.

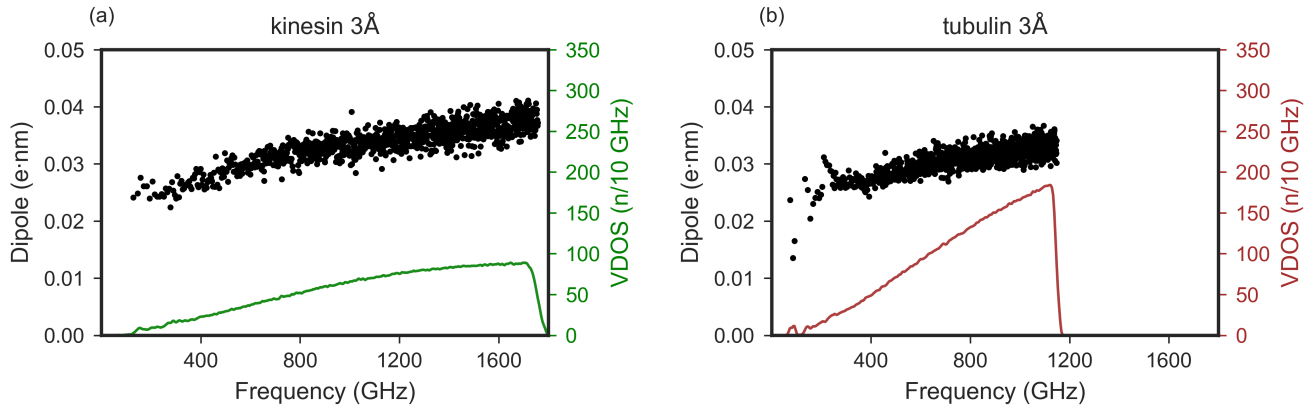

Figure S1-2. Comparison of variation of dipole of kinesin and tubulin systems (with 3 Å water), showing ρ over frequency for first one thousand modes. Each dot in the figure represent variation of dipole moment and frequency of a particular mode (averaged over 92 calculations). The green and brown curves indicate the number of modes per frequency bin for kinesin and tubulin system(bin size = 10 GHz).

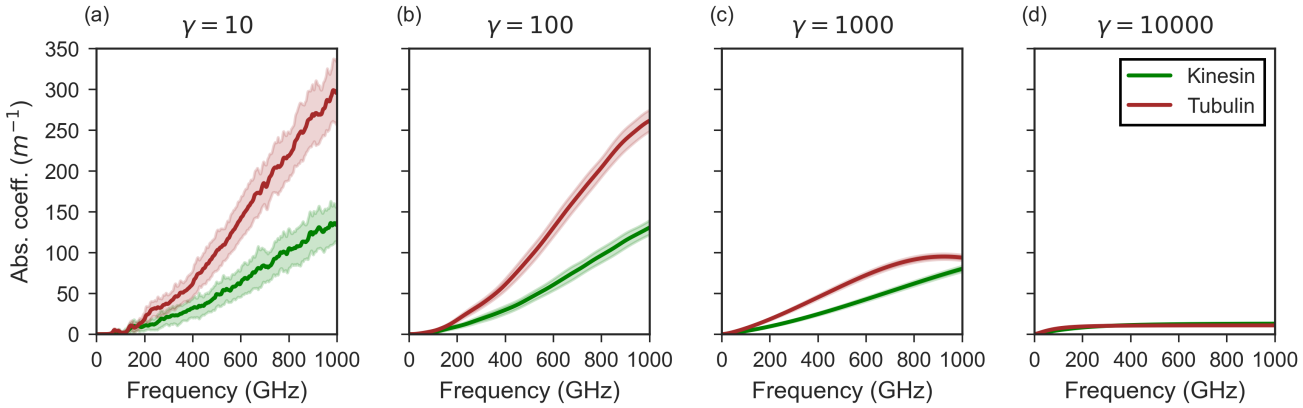

Figure S1-3. Comparison of absorption spectra of kinesin 3 Å and tubulin 3 Å, effect of damping. The concentrations of kinesin and tubulin are 1.9 mg/mL and 5.0 mg/mL, having matching molar concentration of 50 μM

S1-2 Hydration–sequestered water and its impact on χ and α at 100/200 GHz

To estimate how much water is rendered "bound" (and thus effectively removed from bulk THz absorption) by kinesin at the concentrations used, we use the explicit count from our model: the 3 Å hydration shell around kinesin contains $n_b = 1124$ water molecules per protein. For comparison, a solvent–accessible surface area (SASA) estimate using $A_{\text{kinesin,SASA}} = 173$ nm^2 would yield $\sim 1.73 \times 10^3$ waters.

We work in millimolar (mM) units for clarity. Since 1 mM = 1 mol m^{-3}, the protein number density is simply

$$N_V = c_{\text{mM}} N_A. \tag{S1-1}$$

With bulk-water number density $N_{\text{w}} \approx 55.5 \times 10^3\, N_A \simeq 3.34 \times 10^{28}$ m^{-3}, the "removed–water" fraction becomes

$$f_{\text{rm}} \approx \frac{n_b N_V}{N_{\text{w}}} = \left(\frac{n_b N_A}{N_{\text{w}}}\right) c_{\text{mM}} \simeq 0.0203\, c_{\text{mM}}, \tag{S1-2}$$

i.e. $f_{\text{rm}}(\%) \simeq 2.03\, c_{\text{mM}}$.

For the four working concentrations

$$c_{\text{mM}} = \{0.0516,\ 0.155,\ 0.307,\ 0.517\}\ \text{mM} \quad \left(\text{which correspond to } \{1.9,\ 5.7,\ 11.3,\ 19\}\ \text{mg mL}^{-1}\right),$$

Eq. (S1-2) gives

$$f_{\text{rm}} \approx \begin{cases} 0.105\% & c_{\text{mM}} = 0.0516, \\ 0.315\% & c_{\text{mM}} = 0.155, \\ 0.623\% & c_{\text{mM}} = 0.307, \\ 1.050\% & c_{\text{mM}} = 0.517. \end{cases}$$

Relation between susceptibility, refractive index, and absorption

Adopting the $e^{-j\omega t}$ convention, we write

$$\chi(\nu) = \chi'(\nu) + j\chi''(\nu), \qquad m = n + j\kappa = \sqrt{\varepsilon_r}, \qquad \alpha = \frac{4\pi f\, \kappa}{c}. \tag{S1-3}$$

For water near room temperature we use

$$\varepsilon_r(100\ \text{GHz}) \approx 8.9 + j\,14.0, \qquad \varepsilon_r(200\ \text{GHz}) \approx 5.6 + j\,7.0, \tag{S1-4}$$

from a double–Debye description of liquid water[1,2]. Hence,

$$\chi_{\text{w}}(100) \approx 7.9 + j\,14.0, \quad \chi_{\text{w}}(200) \approx 4.6 + j\,7.0,$$

and

$$\alpha_{\text{water}}(100\ \text{GHz}) \approx 8.22 \times 10^3\ \text{m}^{-1}, \qquad \alpha_{\text{water}}(200\ \text{GHz}) \approx 1.09 \times 10^4\ \text{m}^{-1}.$$

These values are consistent with broadband model–measurement intercomparisons in the 31–225 GHz range[3,4].

Bound–water effect as linear mixing

Approximating the "missing–water" effect by dilute linear mixing gives

$$\Delta\chi' \approx -f_{\rm rm}\,\chi'_{\rm w}, \qquad \Delta\chi'' \approx -f_{\rm rm}\,\chi''_{\rm w}, \qquad \Delta\alpha \approx -f_{\rm rm}\,\alpha_{\rm water}. \tag{S1-5}$$

The computed reductions (negative values) are summarized in Table S1-1.

Table S1-1. Estimated reductions in χ' and χ'' and absorption coefficient α due to bound water for kinesin concentrations in mM (corresponding mg/mL in parentheses).

	$f_{\rm rm}$ (%)	$\Delta\chi'(100)$	$\Delta\chi''(100)$	$\Delta\alpha_{100}$ [m^{-1}]	$\Delta\chi'(200)$	$\Delta\chi''(200)$	$\Delta\alpha_{200}$ [m^{-1}]
$c = 0.0516$ mM (1.9 mg mL^{-1})	0.105	-0.0083	-0.0147	-8.63×10^{0}	-0.0048	-0.0073	-1.14×10^{1}
$c = 0.155$ mM (5.7 mg mL^{-1})	0.315	-0.0249	-0.0441	-2.59×10^{1}	-0.0145	-0.0221	-3.43×10^{1}
$c = 0.307$ mM (11.3 mg mL^{-1})	0.623	-0.0491	-0.0870	-5.11×10^{1}	-0.0286	-0.0435	-6.73×10^{1}
$c = 0.517$ mM (19 mg mL^{-1})	1.050	-0.0830	-0.146	-8.59×10^{1}	-0.048	-0.073	-1.14×10^{2}

These values scale linearly with the assumed shell thickness and n_b. Because bound water retains a diminished and shifted dielectric response[5], the numbers above represent upper bounds on the reduction to the bulk–water contribution in χ and α at 100–200 GHz. Permittivity and absorption values are taken from double–Debye fits to liquid water[1,2].

When do 3 Å hydration shells begin to overlap?

Using again $n_b = 1124$ waters per protein and the number density of bulk water $N_{\rm w}^{(\rm num)} \approx 33.4$ nm^{-3}, the shell volume is

$$V_{\rm shell} \approx \frac{1124}{33.4} \simeq 33.6\ {\rm nm}^3. \tag{S1-6}$$

With specific volume $\bar{v} \approx 0.73$ mL g^{-1} and $M = 36.8$ kDa, the protein volume is

$$V_{\rm prot} \approx 44.6\ {\rm nm}^3. \tag{S1-7}$$

The combined 3 Å-expanded (core + shell) "exclusion" volume is

$$V_{3\text{Å}} \approx 78.2\ {\rm nm}^3, \qquad r_{\rm eff} \approx 2.65\ {\rm nm}. \tag{S1-8}$$

A touching criterion $d \approx 2r_{\rm eff}$ implies

$$N_V^{(\rm touch)} \approx \frac{1}{(2r_{\rm eff})^3} \simeq 6.7\times10^{24}\ {\rm m}^{-3}, \qquad c_{\rm overlap}^{(\rm touch)} \approx 0.41\ {\rm g\,mL}^{-1}. \tag{S1-9}$$

Bracketing by volume fraction $\phi = N_V V_{3\text{Å}}$, we obtain:

$$\text{Continuum percolation (overlapping spheres), } \phi_c \approx 0.289[6]: \quad c \approx 0.29\,\frac{M/N_A}{V_{3\text{Å}}} \simeq 2.3\times10^{2}\ {\rm mg\,mL}^{-1}, \tag{S1-10}$$

$$\text{Random close packing (hard spheres), } \phi \approx 0.64[7]: \quad c \approx 0.64\,\frac{M/N_A}{V_{3\text{Å}}} \simeq 5.0\times10^{2}\ {\rm mg\,mL}^{-1}, \tag{S1-11}$$

$$\text{Space filling, } \phi = 1: \quad c \approx \frac{M/N_A}{V_{3\text{Å}}} \simeq 7.8\times10^{2}\ {\rm mg\,mL}^{-1}. \tag{S1-12}$$

Using the explicit $n_b = 1124$ waters in the 3 Å shell, hydration shells begin to geometrically overlap at concentrations of order

$$c \sim 0.3\text{–}0.5\ {\rm g\,mL}^{-1}, \quad \text{central estimate: } c_{\rm overlap} \approx 0.41\ {\rm g\,mL}^{-1}.$$

Our working concentrations 0.051–0.517 mM (i.e. 1.9–19 mg mL^{-1}) are well below this range, so shell–shell overlap should be rare under those conditions.

References

1. Meissner, T. & Wentz, F. The complex dielectric constant of pure and sea water from microwave satellite observations. *IEEE Transactions on Geoscience and Remote Sensing* **42**, 1836–1849 (2004).
2. Ellison, W. J. Permittivity of Pure Water, at Standard Atmospheric Pressure, over the Frequency Range 0–25THz and the Temperature Range 0–100°C. *Journal of Physical and Chemical Reference Data* **36**, 1–18 (2007).
3. Kneifel, S. *et al.* Absorption Properties of Supercooled Liquid Water between 31 and 225 GHz: Evaluation of Absorption Models Using Ground-Based Observations (2014). Section: Journal of Applied Meteorology and Climatology.
4. Turner, D. D., Kneifel, S. & Cadeddu, M. P. An Improved Liquid Water Absorption Model at Microwave Frequencies for Supercooled Liquid Water Clouds (2016). Section: Journal of Atmospheric and Oceanic Technology.
5. Charkhesht, A., Regmi, C. K., Mitchell-Koch, K. R., Cheng, S. & Vinh, N. Q. High-Precision Megahertz-to-Terahertz Dielectric Spectroscopy of Protein Collective Motions and Hydration Dynamics. *The Journal of Physical Chemistry B* **122**, 6341–6350 (2018).
6. Torquato, S. & others. *Random heterogeneous materials: microstructure and macroscopic properties*, vol. 16 (Springer, 2002).
7. Bernal, J. D. The Bakerian lecture, 1962. The structure of liquids. *Proceedings of the Royal Society of London. Series A, Mathematical and Physical Sciences* **280**, 299–322 (1964). Publisher: JSTOR.